Inorganic Chemistry

Article

pubs.acs.org/IC

Phenolate- and Acetate (Both μ_2-1,1 and μ_2-1,3 Modes)-Bridged Linear Co^{II}_3 and $Co^{II}_2Mn^{II}$ Trimers: Magnetostructural Studies

Anuj Kumar Sharma,[†] Francesc Lloret,[‡] and Rabindranath Mukherjee*[,†,§]

[†]Department of Chemistry, Indian Institute of Technology Kanpur, Kanpur 208 016, India

[‡]Departament de Quımíca, Inorgànica/Instituto de Ciencia Molecular (ICMOL), Universitat de Valeńcia, Polígono de la Coma, s/n, 46980-Paterna (València), Spain

Supporting Information

ABSTRACT: A full report on the synthesis, crystal structure, spectroscopic characterization, and magnetic properties of two new trinuclear complexes (one homo- and another heterotrinuclear) $[(L)_2Co^{II}_3(OAc)_4(MeOH)_2]\cdot 6MeOH$ (**1**) and $[(L)_2Co^{II}_2Mn^{II}(OAc)_4(MeOH)_2]\cdot 6MeOH$ (**2**) [HL = *N*-methyl-*N*-2-hydroxybenzyl-2-aminoethyl-2-pyridine] is presented. The properties of **1** and **2** are compared to that of three previously communicated complexes $[(L)_2Ni^{II}_3(OAc)_4(MeOH)_2]\cdot 6MeOH$ (**3**), $[(L)_2Ni^{II}_2Mn^{II}(OAc)_4(H_2O)_2]$ (**4**), and $[(L)_2Ni^{II}_2Co^{II}(OAc)_4(MeOH)_2]\cdot 6MeOH$ (**5**) (*Inorg. Chem.* **2007**, *46*, 5128−5130). All are centrosymmetric trimers with the central metal ion situated on an inversion center. Adjacent metal ions are triply bridged by a μ_2-phenolate and two acetate (one in μ_2-1,1 mode and another in μ_2-1,3 mode) groups. Magnetic investigations reveal that the complexes are ferromagnetically coupled (J in cm^{-1}): +1.20 (**1**) and +0.71 (**2**). The reported J values are +1.10 (**3**), −0.30 (**4**), and +1.06 (**5**). It reveals that total spins are as follows: S = 9/2 (**1**), 11/2 (**2**), 3 (**3**), 1/2 (**4**), 7/2 (**5**). The role of M−O(μ_2-phenoxide)−M′, M−O(μ_2-1,1-acetate)−M′, and M−O(μ_2-1,3-acetate)−M′ (M = M′ = Co^{II}, Ni^{II}; M = Co^{II}, M′ = Mn^{II}; M = Ni^{II}, M′ = Mn^{II}, Co^{II}) bond angles on the observed magnetic behavior has been noted.

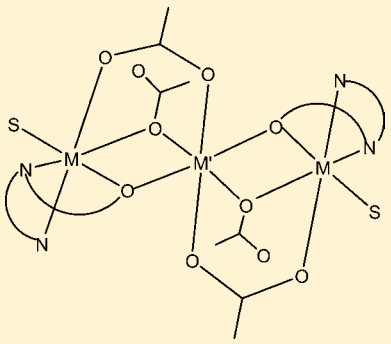

INTRODUCTION

Tuning the magnetic properties of transition-metal complexes with various metal site geometry and varying nuclearity has been a subject of great interest for synthetic inorganic chemists. Consequently, during the past three decades, a large number of polynuclear transition-metal complexes have been synthesized, and their magnetic properties have been studied in detail.[1−3] A major thrust of research in the interdisciplinary area of molecular magnetism[2] is understanding the mechanism of spin-coupling and to arrive at meaningful magnetostructural correlations,[3] from studies of discrete molecules, and utilization of derived ideas in large clusters to search for molecule-based magnetic materials.[4]

It is understandable that the ligand disposition around paramagnetic metal ions, and the nature and disposition (bridging angles) of the bridging atoms/groups (acetates,[5] azide,[6] alkoxides,[3c] and phenolates[3e,f,h−j] are commonly used bridging groups) influence magnetic-exchange interactions. From this standpoint, we initiated a program[7] to systematically synthesize and investigate magnetic-exchange interactions in 1-D coordination polymers, and tetra- and hepta-metal clusters supported by (2-pyridyl)alkylamine-appended carboxylate ligands.

The nature and magnitude of the magnetic-exchange interaction in heterobridged complexes are governed by the structural and electronic behavior of different types of bridges. Notably, a number of homo- and heterotrinuclear complexes[3i,8−21] supported by phenol-based chelating ligands (*salen*-type tetradentate terminal and bridging ligands in particular) with or without additional acetate bridging in the μ_2-1,1- and μ_2-1,3-modes have been studied, because of their interesting magnetic behavior. Face-sharing systems are of special importance in understanding overlapping magnetic orbitals, because both $d_{x^2-y^2}$ and d_{z^2} orbitals are involved in bridging interaction. In view of the above, the preparation of complexes with new chelating ligands to create new homo- and heterotrinuclear magnetic material to arrive at any meaningful magnetostructural trend is a challenge.

Among other heterobridge combinations, indigenous alkoxide/phenoxide and exogenous acetate and azide in various coordination modes are very popular. Understanding the magnetic-exchange interaction mediated by a combination of two bridges, phenolate and acetate, with the latter in its different bridging modes (μ_2-1,1 and μ_2-1,3) in homo- or heterotrinuclear complexes is not straightforward, as all of these bridges may either reinforce (complementarity) or counterbalance (counter-complementarity) their effects.[22,23] The presence of such heterobridges in one system is an interesting approach not only for constructing new materials but also for modulating magnetic properties in a controlled manner, as both of these bridging functionalities can transmit ferro- or antiferromagnetic exchange-coupling between transition metal centers.

Received: October 15, 2012
Published: April 11, 2013

   dx.doi.org/10.1021/ic302259t | *Inorg. Chem.* 2013, 52, 4825−4833

Table 1. Data Collection and Structure Refinement Parameters for $[(L)_2Co^{II}_3(OAc)_4(MeOH)_2]\cdot 6MeOH$ (1), $[(L)_2Co^{II}_2Mn^{II}(OAc)_4(MeOH)_2]\cdot 6MeOH$ (2), and $[(L)Ni^{II}(OBz)(MeOH)(H_2O)]$ (6)

	1	2	6
chem formula	$C_{46}H_{76}N_4O_{18}Co_3$	$C_{46}H_{64}N_4O_{18}Co_2Mn$	$C_{23}H_{26}N_2O_5Ni$
fw	1149.90	1133.81	471.18
cryst color, habit	pink, block	pink, block	green, block
temp/K	100(2)	100(2)	100(2)
α/Å	0.71069	0.71069	0.71073
cryst syst	triclinic	triclinic	monoclinic
cryst size/mm × mm × mm	0.2 × 0.2 × 0.1	0.3 × 0.2 × 0.2	0.2 × 0.1 × 0.1
space group (No.)	$P\bar{1}$ (No. 2)	$P\bar{1}$ (No. 2)	$P2_1/c$ (No. 14)
a/Å	9.453(5)	9.454(5)	9.8785(12)
b/Å	11.049(5)	11.068(5)	18.663(2)
c/Å	13.381(5)	13.418(5)	12.5431
α/deg	80.237(5)	79.839(5)	
β/deg	82.414(5)	82.283(5)	107.545(2)
γ/deg	86.047(5)	85.919(5)	
V/Å^3	1363.7(11)	1367.9(11)	2204.8(5)
Z	1	1	4
d_{calcd}/g cm^{-3}	1.400	1.376	1.419
μ/mm^{-1}	0.973	0.897	0.917
no. reflns collected	9203	9054	12 281
no. unique reflns	6503 (R_{int} = 0.0195)	6428 (R_{int} = 0.0177)	5417 (R_{int} = 0.1143)
no. reflns used [$I > 2\sigma(I)$]	5451	5315	2719
GOF on F^2	1.044	1.105	0.992
final R indices [$I > 2\sigma(I)$]	0.0464[a] (0.1262[b])	0.0536[a] (0.1130[b])	0.0785[a] (0.1752[b])
R indices (all data)	0.0560[a] (0.1321[b])	0.0753[a] (0.1561[b])	0.1718[a] (0.2420[b])

[a] $R_1 = \sum(|F_o| - |F_c|)/\sum|F_o|$. [b] $wR_2 = \{\sum[w(|F_o|^2 - |F_c|^2)^2]/\sum[w(|F_o|^2)^2]\}^{1/2}$.

Keeping the above-mentioned facts in mind, we initiated a program to systematically investigate the magnetic properties of a series of phenolate- and acetate-bridged homo- and heterotrinuclear complexes. The major aims of the present study are (i) to synthesize a class of triply heterobridged [μ_2-phenolate- and acetate-bridged (both μ_2-1,1- and μ_2-1,3-modes)] homo- and heterotrinuclear complexes with a common (2-pyridyl)ethylamine-based phenolate ligand, (ii) to obtain a Co^{II}_3 complex with high-spin Co^{II} as it is strongly anisotropic with three-unpaired electrons (S = 3/2), (iii) to obtain a $Co^{II}_2Mn^{II}$ complex, combining anisotropy of Co^{II} with high-spin Mn^{II}, which is isotropic with five-unpaired electrons (S = 5/2), and (iv) to compare the magnetostructural properties of these two systems with three homo- and heterotrinuclear complexes Ni^{II}_3, $Ni^{II}_2Mn^{II}$, and $Ni^{II}_2Co^{II}$, with 1−1−1, 1−5/2−1, and 1−3/2−1 spin−spin interaction, respectively.[24] The two new complexes have closely related crystal structures and exhibit the 3/2−3/2−3/2 and 3/2−5/2−3/2 spin−spin interactions.

Specifically, we report on the synthesis, crystal structure, and magnetic properties of two new homo- and heterotrinuclear complexes $[(L)_2Co^{II}_3(OAc)_4(MeOH)_2]\cdot 6MeOH$ (**1**) and $[(L)_2Co^{II}_2Mn^{II}(OAc)_4(MeOH)_2]\cdot 6MeOH$ (**2**), along with comparative studies on our previously communicated series[24] of complexes $[(L)_2Ni^{II}_2M^{II}(\mu_2\text{-}1,3\text{-}OAc)_2(\mu_2\text{-}1,1\text{-}OAc)_2(S)_2]\cdot x MeOH$ [HL = *N*-methyl-*N*-2-hydroxybenzyl-2-aminoethyl-2-pyridine; M = Ni, S = MeOH, x = 6 (**3**); M = Mn, S = H_2O, x = 0 (**4**); M = Co, S = MeOH, x = 6 (**5**)]. To understand the trinucleation process, we synthesized and structurally characterized a mononuclear precursor complex $[(L)Ni^{II}(OBz)(MeOH)(H_2O)]$ (**6**), which is also reported here.

EXPERIMENTAL SECTION

Reagents and Materials. All reagents were obtained from commercial sources and used as received. Solvents were dried/purified as reported previously.[7,24] 2-(Bromomethyl)phenylacetate was prepared following a reported procedure.[25] The ligand and the complexes **3**−**5** were prepared as described previously.[24]

Syntheses of Complexes. *$[(L)_2Co^{II}_3(OAc)_4(MeOH)_2]\cdot 6MeOH$ (**1**).* To a solution of HL (0.2 g, 0.826 mmol) in MeOH (10 mL) was added $Co^{II}(OAc)_2\cdot 4H_2O$ (0.310 g, 1.24 mmol), and the mixture was refluxed for 1 h. Upon cooling, the pink crystalline solid that formed was filtered, washed with cold MeOH, and dried in vacuum. Yield: 0.245 g, 60%. Recrystallization from hot MeOH afforded single crystals suitable for X-ray structural studies. Anal. Calcd for $C_{46}H_{78}N_4O_{18}Co_3$: C, 47.96; H, 6.78; N, 4.86. Found: C, 47.56; H, 6.96; N, 5.06. IR (KBr, cm^{-1}, selected peaks): 3381 (ν(OH)), 1570 (m, ν_{asym}(CO), 1422 (s, ν_{sym}(CO)), 1293 (ν(PhO$^-$)). Absorption spectrum [λ_{max}, nm (ε, M^{-1} cm^{-1})] (in MeOH): 240 (16 500), 265 sh (11 200), 285 sh (6900), 370 sh (640), 470 sh (70), 495 sh (80), 510 (70).

*$[(L)_2Co^{II}_2Mn^{II}(OAc)_4(MeOH)_2]\cdot 6MeOH$ (**2**).* $Co^{II}(OAc)_2\cdot 4H_2O$ (0.205 g, 0.826 mmol) and $Mn^{II}(OAc)_2\cdot 4H_2O$ (0.101 g, 0.413 mmol) were dissolved in MeOH (10 mL). To this mixture was added a solution of HL (0.2 g, 0.826 mmol) dissolved in MeOH (2 mL) dropwise. The solid that precipitated out after 15 min was filtered, washed with MeOH, and dried in vacuum. Yield: 0.185 g, 50%. Recrystallization from hot MeOH afforded single crystals suitable for X-ray diffraction studies. Anal. Calcd for $C_{46}H_{78}N_4O_{18}Co_2Mn$: C, 49.23; H, 5.40; N, 6.05. Found: C, 49.12; H, 5.62; N, 6.11. IR (KBr, cm^{-1}, selected peaks): 3420 (ν(OH)), 1579 (m, ν_{asym} (CO)), 1420 (s, ν_{sym}(CO)), 1304 (ν(PhO$^-$)). Absorption spectrum [λ_{max}, nm (ε, M^{-1} cm^{-1})] (in MeOH): 240 (20 600), 290 sh (8000), 390 sh (370), 620 sh (70), 1060 (40).

*$[(L)Ni^{II}(OBz)(MeOH)(H_2O)]$ (**6**).* To a solution of HL (0.2 g, 0.826 mmol) in MeOH (3 mL) was added an aqueous solution (3 mL) of $[Ni^{II}(H_2O)_6](ClO_4)_2$ (0.306 g, 0.83 mmol). The green solution thus obtained was stirred for 5 min. Next, an aqueous solution (5 mL) of sodium benzoate (0.233 g, 1.65 mmol) was added. The solid that

dx.doi.org/10.1021/ic302259t | Inorg. Chem. 2013, 52, 4825−4833

Scheme 1. Proposed Reaction Sequence for Formation of the Trimers

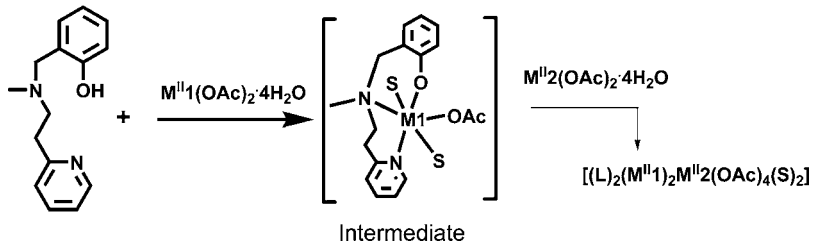

formed immediately was filtered, washed with water, and dried under vacuum. Yield: 0.18 g, 46%. Single crystals suitable for X-ray diffraction were obtained by vapor diffusion of Et_2O into a MeOH solution of the complex. Anal. Calcd for $C_{23}H_{28}N_2O_5Ni$: C, 58.63; H, 5.99; N, 5.95. Found: C, 58.12; H, 5.72; N, 6.21. IR (KBr, cm^{-1}, selected peaks): 1599, 1557 ν_{asym}(CO), 1482, 1447 (ν_{sym} (CO)), 1395 (ν(PhO$^-$)). Absorption spectrum [λ_{max}, nm (ε, M^{-1} cm^{-1})] (in MeOH): 260 sh (7000), 290 sh (3500), 390 sh (40), 660 (10), 1060 (7).

Physical Measurements. Elemental analyses (C, H, N) were obtained using Thermo Quest EA 1110 CHNS-O, Italy. Spectroscopic measurements were made using the following instruments: IR (KBr, 4000−600 cm^{-1}), Bruker Vector 22; electronic, Perkin-Elmer Lambda 2 and Agilent 8453 diode-array spectrophotometer; X-band EPR, Varian 109 C and Bruker EMX 1444 spectrometers (fitted with a quartz Dewar for measurement at 120 K). ^{1}H NMR spectra were obtained on JEOL JNM LA 400 (400 MHz) spectrometer using $CDCl_3$ solutions. Chemical shifts (in ppm) are reported with reference to TMS. The measurements were carried out using a Quantum Design SQUID magnetometer (Valéncia) at 0.1 T for T < 50 K to avoid saturation effects and 0.01 T for T > 50 K. Diamagnetic corrections were estimated from Pascal's constants.[27]

Atomic absorption spectrometry (AAS) measurements were done using a SpectrAA 220FS atomic absorption spectrometer (VARIAN). X-ray powder diffraction (XRPD) of **1** and **2** were recorded on a Bruker D8 Advance Series-2 powder X-ray diffractometer, operated at 30 kV and 20 mA, using a Cu-target tube and a graphite monochromator. The intensity data were recorded by continuous scan in a 2I/I mode from 6° to 50° with a step size of 0.05° and a scan speed of 3° min^{-1}. Simulation of the XRPD spectra was carried out using single-crystal data and diffraction-crystal module of the Mercury (Hg) program available free of charge via the Internet at http://www.iucr.org.

Crystallographic Refinement and Structure Solution. Single crystals of suitable dimensions were used for data collection. Diffraction intensities were collected on a Bruker SMART APEX CCD diffractometer, with graphite-monochromated Mo Kα (λ = 0.71073 Å) radiation at 100(2) K. For data reduction, the "Bruker Saint Plus" program was used. The data were corrected for Lorentz and polarization effects; empirical absorption correction (SADABS) was applied. Structures were solved by SIR-97 and refined by full-matrix least-squares methods based on F^2 using SHELXL-97, incorporated in WinGX 1.64 crystallographic collective package.[28] The positions of the hydrogen atoms were calculated by assuming ideal geometries but not refined. For compound **2**, some degree of disorder was encountered with one of the oxygen atoms of one solvent (MeOH) molecule. One oxygen atom of one MeOH was displaced over two positions, and they were refined with a site occupation factor of 0.85/0.15, and a few reflections of bad quality were omitted to get a better structure solution. Pertinent crystallographic parameters for **1**, **2**, and **6** are summarized in Table 1. CCDC-904906 (**1**), 904907 (**2**), 656732 (**3**), 656733 (**4**), 656734 (**5**), and 904908 (**6**) contain the supplementary crystallographic data for this Article. These data can be obtained free of charge from The Cambridge Crystallographic Data Centre via www.ccdc.cam.ac.uk/data_request/cif.

RESULTS AND DISCUSSION

Syntheses. We demonstrated in our earlier communication[24] that the deprotonated tridentate ligand L$^-$ affords trinuclear complexes on reaction with 3d metal acetates. Homo- and heterotrinuclear complexes of pertinence to this work [(L)$_2$(M1^{II})$_2$M2^{II}(μ_2-1,1-OAc)$_2$(μ_2-1,3-OAc)$_2$(S)$_2$] (M1^{II} = Co, Ni; M2^{II} = Mn, Co, Ni; S = MeOH, H_2O) have been obtained by the reaction in MeOH of HL and a mixture of M^{II}(OAc)$_2$·4H_2O (M = Co, Ni) (ligand:metal in 2:3 mole ratio for homonuclear complexes) and M^{II}(OAc)$_2$·4H_2O (M = Mn, Co) (ligand:M1:M2 in 2:2:1 mole ratio for heteronuclear complexes). Thus, the synthetic route has been applied successfully yielding the first linear trinuclear complexes supported by μ_2-phenoxide, μ_2-1,1-acetate, and μ_2-1,3-acetate heterobridges. We believe that the trinuclear core is assembled as per the reaction sequence depicted in Scheme 1. It is invoked that first a mononuclear intermediate of M1 is formed, in which the coordinated phenolate and acetate ions have residual electron density for further reaction. Two such mononuclear units in turn react with M2 acetate and afford homo/hetero-trinuclear core, through phenolate and acetate bridges. This conjecture is supported by the synthesis and structural characterization of a mononuclear complex [(L)Ni^{II}(OBz)-(MeOH)(H_2O)] (**6**), when sodium benzoate was used as the carboxylate source.

Elemental analysis and spectral (IR and UV−vis) data are in agreement with the above formulations of the complexes **1**, **2**, and **6**. The complexes are not readily soluble in common organic solvents but on warming dissolve in MeOH. The structures of all three complexes have been authenticated by X-ray crystallography.

To analyze the purity of heterometallic complexes, atomic absorption spectroscopy was used to determine the concentration of metal ions present in the complexes. For the heterometallic complex **2**, the ratio of concentration of the terminal (Co^{II}) and the central metal (Mn^{II}) should be 2:1. The results obtained justified the purity of samples.

X-ray powder diffraction analyses were also performed to ensure that the trinuclear core is the sole species present as bulk material. The experimental and computer simulated XRPD patterns of **1** and **2** are shown in Figures S1, S2, Supporting Information. Although the experimental patterns have a few unindexed diffraction lines in comparison with those simulated, still it can confidently be claimed that the bulk samples of **1** and **2** are pure homo- and heterotrinuclear complexes, respectively.

Spectroscopic Characterization. For all of the complexes, the broad IR absorption at ∼3400 cm^{-1} is attributed to O−H stretching frequency of MeOH or H_2O. In addition, the band at ∼1300 cm^{-1} is assigned to ν(C−O) of the coordinated phenolate group. The absorption at 1257 cm^{-1} is assigned to the phenol group, which was shifted to ∼1300 cm^{-1} in the metal complexes, as the ligand coordinates in its deprotonated

dx.doi.org/10.1021/ic302259t | Inorg. Chem. 2013, 52, 4825−4833

form. The broad absorptions at ∼1580 and at ∼1420 cm^{-1} are attributed to asymmetric and symmetric ν(CO) stretching frequency of the acetate group, respectively.

In the UV−vis spectra of **1**, **2**, and **6** in MeOH (Figures S3−S5, Supporting Information), absorption bands at ∼240 and ∼280 nm are observed due to intraligand transitions. Complexes **1** and **2** exhibit multiple transitions at ∼500 nm, which are assigned as due to $^4T_1g(F) \rightarrow {}^4A_2g(F)$ and $^4T_1g(F) \rightarrow {}^4T_1g(P)$, associated with high-spin octahedral cobalt(II) parentage.[7,29,30] Three spin-allowed d−d transitions are expected for octahedral Co^{II}, unless the field-strength of the ligands is such that the $^4A_{2g}$ and $^4T_{1g}(P)$ terms have the same energy. This occurs when the two states cross. The effect of incorporation of Mn^{II} (S = 5/2) center between the two Co^{II} centers (S = 3/2) in **2** can easily be recognized looking at the electronic spectrum of the complex. The split band at ∼500 nm disappears in **2**, and a shoulder at 620 nm is observed. For Ni^{II}_3, $Ni^{II}_2Mn^{II}$, and $Ni^{II}_2Co^{II}$ complexes[24] and complex **6** (Figure S5), absorption bands at ∼1060, ∼655, and ∼390 nm are assigned due to three spin-allowed transitions $^3A_{2g}(F) \rightarrow {}^3T_{2g}(F)$, $^3A_{2g}(F) \rightarrow {}^3T_{1g}(F)$, and $^3A_{2g}(F) \rightarrow {}^3T_{1g}(P)$, respectively, associated with octahedral Ni^{II} ion.[29,30] For these complexes, a weak absorption band is clearly observable at ∼780 nm, which is due to the spin-forbidden transition $^3A_{2g} \rightarrow {}^1E_{1g}$.

Description of the Structures of 1 and 2. Perspective views of the metal coordination environment of $[(L)_2Co^{II}_3(OAc)_4(MeOH)_2]\cdot 6MeOH$ (**1**) and $[(L)_2Co^{II}_2Mn^{II}(OAc)_4(MeOH)_2]\cdot 6MeOH$ (**2**) are presented in Figure S6 and Figure 1, respectively. The unit cells of **1** and **2** in the $P\bar{1}$ space

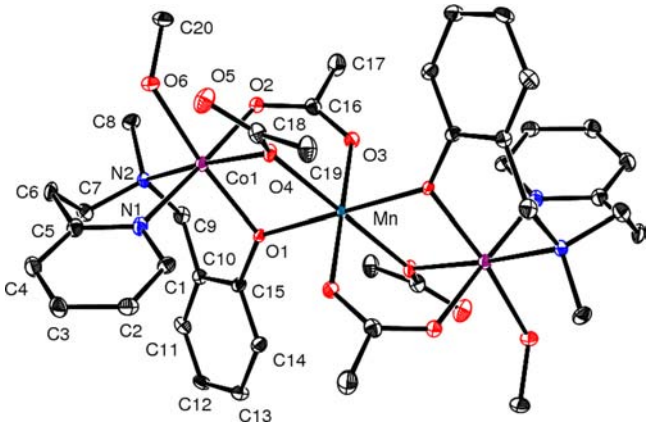

Figure 1. Perspective view of metal-coordination environment in the crystal of $[(L)_2Co^{II}_2Mn^{II}(OAc)_4(MeOH)_2]\cdot 6MeOH$ (**2**).

group (Table 1) are isostructural, containing centrosymmetric trimers. The central M^{II} ion (Co2 in **1**; Mn in **2**) is situated on an inversion center, forming linear Co^{II}_3 and $Co^{II}_2Mn^{II}$ trinuclear complexes. The bond lengths and bond angles of **1** and **2** are given in Table 2. The terminal M^{II} ions [M(1) and M(1′)] are coordinated by a pyridyl nitrogen N1, a tertiary amine nitrogen N2, a bridging phenolate oxygen atom O1 from L^-, two bridging carboxylate oxygen atoms [O2 of μ-1,3-bridging and O4 of μ-1,1-monatomic bridging mode], and an oxygen atom O6 of coordinated MeOH molecule. Thus, the inversion-related terminal Co^{II} ions have a pseudo-octahedral coordination. The coordination around the central M^{II} ion is also pseudo-octahedral involving a bridging phenolate oxygen atom O1, two bridging carboxylate oxygen atoms [O3 of μ-1,3-

Table 2. Selected Bond Lengths (Å) and Bond Angles (deg) for $[(L)_2Co^{II}_3(OAc)_4(MeOH)_2]\cdot 6MeOH$ (1) and $[(L)_2Co^{II}_2Mn^{II}(OAc)_4(MeOH)_2]\cdot 6MeOH$ (2)

	1	2
M1−N1	2.157(2)	2.167(3)
M1−N2	2.175(2)	2.172(3)
M1−O1	2.0028(18)	2.006(3)
M1−O2	2.0829(19)	2.088(3)
M1−O4	2.1884(19)	2.190(3)
M1−O6	2.1360(19)	2.140(3)
M2−O1	2.0716(18)	2.106(3)
M2−O3	2.0530(19)	2.094(3)
M2−O4	2.1678(18)	2.194(3)
M1···M2	3.1637(9)	3.1873(9)
	1	**2**
N1−M1−N2	89.90(8)	89.66(12)
N1−M1−O1	91.23(8)	91.29(12)
N1−M1−O2	177.93(7)	177.85(12)
N1−M1−O4	91.04(7)	90.57(11)
N1−M1−O6	87.68(8)	87.56(12)
N2−M1−O1	94.68(7)	94.71(11)
N2−M1−O2	89.90(8)	90.72(11)
N2−M1−O4	174.78(7)	175.54(11)
N2−M1−O6	97.53(7)	97.39(12)
O1−M1−O2	90.76(8)	90.79(11)
O1−M1−O4	80.17(7)	80.83(10)
O1−M1−O6	167.73(7)	167.84(11)
O2−M1−O4	88.72(7)	89.22(10)
O2−M1−O6	90.26(8)	90.29(11)
O4−M1−O6	87.63(7)	87.07(10)
O1−M2−O3	87.67(7)	87.10(10)
O1−M2−O3[a]	92.33(7)	92.90(10)
O1−M2−O4	79.17(7)	78.58(10)
O1−M2−O4[a]	100.83(7)	101.42(10)
O3−M2−O4	89.56(7)	88.94(11)
O3−M2−O4[a]	90.44(7)	91.06(11)
M1−O1−M2	101.864(18)	101.623(17)
M1−O4−M2	93.141(16)	93.289(15)

[a]Symmetry operator for the generated atoms: $-x+1, -y+1, -z+2$ for **1**; $-x+1, -y+1, -z+1$ for **2**.

bridging and O4 of μ-1,1-monatomic bridging mode], and their symmetry-related ones. Thus, the three pseudo-octahedral M^{II} ions form a linear array with two terminal moieties in a facial N_2O donor set from L^-. The coordination spheres of terminal and central M^{II} ions are, however, severely distorted from ideal octahedral geometry. The angles between trans atoms at the terminal Co^{II} centers are in the range 167.73(7)−177.93(7)° for **1** and 167.84(11)−177.85(12)° for **2**. The cis angles span a wide range 80.17(7)−97.53(7)° for **1** and 80.83(10)−97.39(12)° for **2**. The distances between the terminal-central M^{II} ions are 3.164(1) Å for **1** and 3.187(9) Å for **2**, and between the two terminal M^{II} ions are 6.327(2) Å for **1** and 6.375(2) Å for **2**. The sums of the angles at the phenoxide and monatomic bridging carboxylate oxygens are almost 360° (O1 359.10° and O4 356.43° for **1**; O1 358.99° and O4 356.8° for **2**), indicating almost no pyramidal oxygen distortion. Moreover, the terminal Co^{II} ions are out of the plane defined by N2, O1, O4, and O6 atoms by 0.0034 Å for **1** and by 0.0104 Å for **2** toward the atom O2, attesting that the terminal Co^{II} ions are almost in the equatorial plane. However, the $M^{II}_2O_2$ core is not planar as indicated by the torsional angles [26.441(17)° in **1**

dx.doi.org/10.1021/ic302259t | Inorg. Chem. 2013, 52, 4825−4833

and 27.492(27)° in **2**], defined by the Co1, O1, Co2/Mn, and O4 atoms. The central Co−O and Mn−O bond lengths range from 2.053(2) to 2.168(2) Å and 2.044(3) to 2.194(3) Å, for **1** and **2**, respectively. For both **1** and **2**, the shortest bond is the μ-1,3-acetate oxygen atom O3 and the longest bond is the μ_2-1,1-acetate oxygen atom O4. In **1** the relevant bridging angles Co1−O1−Co2 and Co1−O4−Co2 are 101.86(2)° and 93.14(2)°, respectively. In **2** the corresponding bridging angles Co1−O1−Mn and Co1−O4−Mn are 101.64(2)° and 93.30(1)°, respectively. Complexes **1** and **2** join the rare family of homo- and heterotrinuclear complexes bridged by a μ_2-phenoxide and two acetate (a μ_2-1,1- and a μ_2-1,3-) bridges.[3i,16,24] To the best of our knowledge, **1** and **2** represent the first examples of Co^{II}_3 and $Co^{II}_2Mn^{II}$ complexes in this class of trinuclear complexes.

Crystal Structure of 6. A perspective view of the mononuclear precursor complex $[(L)Ni^{II}(OBz)(MeOH)(H_2O)]$ (**6**) is shown in Figure 2, and selected bond distances

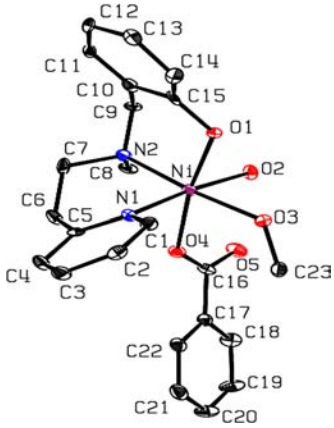

Figure 2. Perspective view of metal-coordination environment in the crystal of $[(L)Ni^{II}(OBz)(MeOH)(H_2O)]$ (**6**).

and angles are collected in Table 3. The Ni^{II} center is coordinated by pyridyl nitrogen N1, amine nitrogen N2, phenolate O1, O2 of water molecule, O3 of MeOH molecule, and benzoate oxygen O4. Thus, it affords a NiN_2O_4 coordination sphere. Appreciable distortions from ideal octahedral geometry are apparent. The angles between trans

Table 3. Selected Bond Lengths (Å) and Angles (deg) in $[(L)Ni^{II}(OBz)(MeOH)(H_2O)]$ (6)

Ni−N1	2.028(4)	N1−Ni−N2	91.8(2)
Ni−N2	2.113(4)	N1−Ni−O1	94.09(18)
Ni−O1	2.137(4)	N1−Ni−O2	174.87(19)
Ni−O2	2.044(4)	N1−Ni−O3	90.58(18)
Ni−O3	2.079(5)	N1−Ni−O4	85.19(18)
Ni−O4	2.109(5)	N2−Ni−O1	93.95(18)
		N2−Ni−O2	91.65(19)
		N2−Ni−O3	174.71(18)
		N2−Ni−O4	96.30(18)
		O1−Ni−O2	89.47(18)
		O1−Ni−O3	81.15(16)
		O1−Ni−O4	169.75(17)
		O2−Ni−O3	86.32(17)
		O2−Ni−O4	90.65(18)
		O3−Ni−O4	88.62(17)

atoms at the metal center are N1−Ni−O2 174.87(19)°, N2−Ni−O3 174.71(18)°, and O1−Ni−O4 169.75(17)°. The cis angle spans a wide range, 81.15(16)−96.30(18)°. The $Ni-N_{py}$ bond length is 2.028(4), and the $Ni-N_{am}$ bond length is 2.113(4) Å. An attracting feature of the structure is that the two solvents H_2O and MeOH are cis to each other, and hence the complex could be useful as a model catalyst for hydrolytic reactions.[31]

Noncovalent Interactions. Careful analysis of the crystal packing of the trinuclear complexes **1**−**5** and the mononuclear complex **6** reveals the presence of extensive noncovalent interactions. In our earlier communication, this aspect for complexes **3**−**5** were not considered.[24] Hydrogen-bonding parameters for **1**−**6** are in Table S1, Supporting Information. In **1** six MeOH molecules are present as solvent of crystallization. Oxygen atom O5 of the μ_2-1,1-acetate group is involved in interaction with O3W−H3W of a MeOH molecule of solvent of crystallization. This MeOH molecule is involved in O−H···O interaction with another MeOH molecule, which has O−H···O interaction with another MeOH molecule. Thus, three MeOH molecules form a linear array due to O−H···O interaction. The oxygen atom O2W of the third MeOH molecule has C−H···O interaction with pyridine 4-H (C3−H3) of a neighboring molecule. In essence, two trimeric units are connected through solvent molecules. These interactions propagate leading to the formation of a 1D chain (Figure S7, Supporting Information).

In **2** the oxygen atom O4 of the μ_2-1,1-acetate group is involved in the C−H···O hydrogen-bonding interaction with pyridine 3-H (C4−H4) of a neighboring molecule (Table S1). This leads to the formation of a 1D chain along the *c*-axis (Figure S8, Supporting Information). In **3** the oxygen atoms O(2) of μ_2-1,3-acetate and O(5) of μ_2-1,1-acetate groups are involved in C−H···O interactions. Oxygen atom O(5) has interaction with pyridine 3-H (C4−H4), which leads to the formation of a 1D chain along the *c*-axis. In addition, O(2) interacts with 4-H of the phenolate ring (C13−H13) and forms a 1D chain along the *a*-axis. Taken together, these interactions lead to the formation of a 2D network structure (Figure S9, Supporting Information). In **4** the oxygen atom O(5) of the μ_2-1,1-acetate group and O(6) of coordinated water molecule are involved in the C−H···O interaction. Oxygen atom O(5) has an additional interaction with 4-H of the pyridine ring (C3−H3) of a neighboring molecule. This leads to the formation of a 1D chain along the *c*-axis. In addition, O(6) has interaction with the methyl group of μ_2-1,3-bridged acetate group (C17−H17A) and forms a 1D chain along *a*-axis. Taken together, such interactions lead to the formation of a 2D network structure (Figure S10, Supporting Information). In **5**, oxygen atom O(5) has interaction with 3-H of the pyridine ring of a neighboring molecule, leading to the formation of a 1D chain along the *c*-axis (Figure S11, Supporting Information). In **6** the presence of C−H···O and C−H···π interactions is observed. Oxygen atom O2 of the coordinated water molecule and O4 from the benzoate group are involved in C−H···O interaction. Oxygen atom O2 is involved in intramolecular interactions with H8B of the N−Me group and also intermolecular hydrogen-bonding interaction with H21 of 3/5-H of the aromatic ring of the benzoate group from other molecule. This leads to the formation of a 1D chain along the *a*-axis (Figure S12, Supporting Information). Moreover, O(4) is involved in bifurcated intramolecular hydrogen-bonding interactions with H6B of py-CH_2CH_2− and H22 of 2/6-H of the aromatic ring of the benzoate group. Intermolecular C−H···π interaction

dx.doi.org/10.1021/ic302259t | Inorg. Chem. 2013, 52, 4825−4833

provides an additional strength to the 1D chain. In fact, C3−H3 of the pyridine ring and π-cloud of the phenolate ring are engaged in interaction at a distance of 2.924 Å.

The C−H···O, O−H···O, and C−H···π hydrogen-bonding parameters observed in this work are in good agreement with literature precedents,[32] including our own findings.[7b,33] These can be classified as intermediate contacts (2.439−2.598 Å), which are appreciably shorter than the sum of van der Waals radii for the H and the neutral O atoms (2.72 Å).[31]

Tribridged Homo- and Heterotrimers. Structural Considerations. It is worth mentioning here that the coordination environments around terminal Ni^{II} ions in **4** and in **3** and **5** are almost identical, the only difference being the presence of H_2O molecule in the place of MeOH.[24]

The bridges present in the reported linear homo- and heterotrinuclear complexes[3i,8−21] with each M^{II} center assuming primarily six-coordination include (i) only acetates, (ii) only μ_2-phenolates, (iii) only μ_2-thiolates, (iv) dibridged, μ_2-phenolate and μ_2-1,3-acetate/benzoate, (v) tribridged, μ_2-phenolate and acetates in both μ_2-1,1- and μ_2-1,3-modes, (vi) tribridged, μ_2-phenolate and acetates in both μ_2-1,1- and μ_2-1,3-modes hydroxamate, and (vii) tribridged, μ_2-phenolate, acetate in μ_2-1,3-mode, and μ_2-1,1-azide. Thus, although a sizable number of linear homo- and heterotrinuclear complexes are reported in the literature, the number of linear trinuclear systems in which the central M^{II} center is supported by three different bridging groups (even if two are of the same type but their bridging mode is different) is rather scarce.[3i,16,24] The present complexes therefore deserve attention. The bridging modes present in **1**−**5** and closely similar systems of pertinence to this work are represented in Figure 3.

Magnetism. Because of the presence of unprecedented μ_2-phenoxide and two types of acetato-bridges μ_2-1,1 and μ_2-1,3 between the terminal and the central M^{II} ions in linear trinuclear complexes, we focused on their magnetic behavior. Measurements of the temperature dependence of the susceptibility for **1** and **2** were carried out for solid powdered samples, collected in the temperature range 2−300 K. The $\chi_M T$ versus T data for the $Co^{II}Co^{II}Co^{II}$ system [d^7 (S = 3/2)−d^7 (S = 3/2)−d^7 (S = 3/2)] **1** is shown in Figure 4 as $\chi_M T$ (cm^3 mol^{-1} K) versus T (K) plot. Upon lowering the temperature the $\chi_M T$ value of 8.25 cm^3 mol^{-1} K at room temperature decreases gradually to ∼20 K to a value of 6.77 cm^3 mol^{-1} K, and then increases at low temperatures to a value of 7.53 cm^3 mol^{-1} K. The $\chi_M T$ value at room temperature is greater than that expected for three high-spin Co^{II} ions through the spin-only formula (3 × 1.87 = 5.61 cm^3 mol^{-1} K with g = 2.0). It could be due to the occurrence of an unquenched orbital contribution typical of the $^4T_{1g}$ ground state for octahedral high-spin Co^{II} complexes.[34,35] Applying the general spin Hamiltonian (eq 1) for linear polynuclear Co^{II} complexes[36,37] with an approximation that the magnetic interaction between the terminal Co^{II} centers (6.3270 Å apart) could be neglected [$H = -\{J_{12}(S_1S_2) + J_{23}(S_2S_3) + J_{13}(S_1S_3)\}$, considering $J = J_{12} = J_{23}$ and assuming the interaction between the terminal Co^{II} ions J_{13} = 0; in the absence of clearly defined exchange pathway between the terminal metal ions, it is justifiable[38]], and taking into account the orbital contribution, a good fit of the temperature-dependent magnetic susceptibility data was obtained: α = −1.19, Δ = −839 cm^{-1}, λ = −139 cm^{-1}, J (Co−Co) = +1.20 cm^{-1} (θ = 0 K) or J(Co−Co) = +1.60 cm^{-1} (θ = −0.44 K) (J is positive for a ferromagnet and negative for an antiferromagnet), where λ is the spin−orbit coupling, Δ is the measure of distortion from ideal octahedral geometry around Co^{II} ion, and α is an orbital reduction factor defined as $\alpha = kA$ (the k parameter considers the reduction of the orbital momentum caused by the delocalization of the unpaired electrons, and the parameter A contains the admixture of the upper $^4T_{1g}(^4P)$ state into the $^4T_{1g}(^4F)$ ground state).[36] The value of A is considered as 1.5, which is a usual value for this kind of ligand.[36]

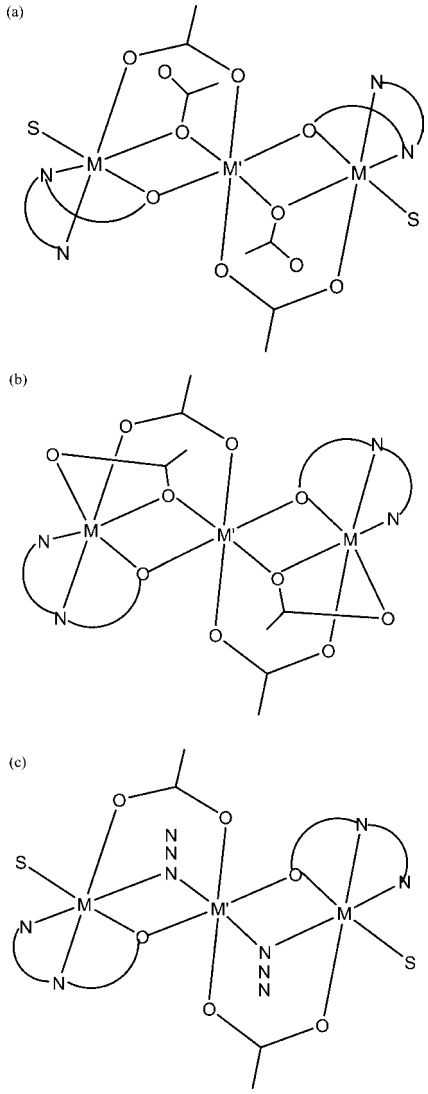

Figure 3. The coordination environment of the M^{II} ions in the linear trimers **1**−**5** (**1** and **3**: M = M′) and reported structures (M = M′ = Ni). (a) This work, (b) (ref 16), and (c) (ref 17).

$$\hat{H} = -\sum_{i=1}^{n} J_i \hat{S}\hat{S}_{i+1} - \sum_{i=1}^{n} \alpha_i \lambda_i \hat{L}_i \hat{S}_i + \sum_{i=1}^{n} \Delta_i [\hat{L}_{zi}^2 - 2/3] + \beta H \sum_{i=1}^{n} (-\alpha_i \hat{L}_i + g_e \hat{S}_i) \quad (1)$$

The $\chi_M T$ versus T plot for $Co^{II}Mn^{II}Co^{II}$ [d^7 (S = 3/2)−d^5 (S = 5/2)−d^7 (S = 3/2)] **2** is also shown in Figure 4. It is noticeable that the nature of the plot is similar to that of **1**. However, the overall values of $\chi_M T$ are higher for **2** because of the presence of high-spin (HS) Mn^{II} central metal ion with five unpaired spins as compared to three (Co^{II} HS) in **1**. The $\chi_M T$

dx.doi.org/10.1021/ic302259t | Inorg. Chem. 2013, 52, 4825−4833

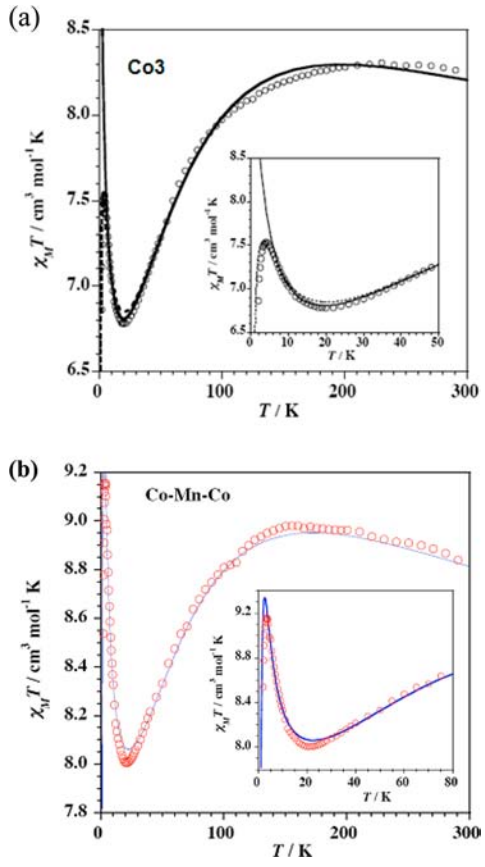

Figure 4. Plot of $\chi_M T$ versus T for **1** and **2**. The behavior below 50 K (for **1**) and below 80 K (for **2**) is presented in an inset.

value of 8.81 cm^3 mol^{-1} K at 300 K upon decreasing the temperature increases gradually to 8.91 cm^3 mol^{-1} K at 160 K, then decreases to a $\chi_M T$ value of 8.02 cm^3 mol^{-1} K, and again it increases sharply below ∼20 K to the $\chi_M T$ value of 9.16 cm^3 mol^{-1} K. Applying the appropriate spin Hamiltonian, considering the anisotropy associated with HS Co^{II} ion and isotropic HS Mn^{II} ion, a good fit of the temperature-dependent magnetic susceptibility data was obtained: $\alpha = 1.27(1)$ ($A = 1.5$, $k = 0.85$, $\lambda = -103(2)$ cm^{-1}, J(Co−Mn) = +0.71(1) cm^{-1}, g(Mn) = 2.0 (fixed), $\theta = -0.70(2)$ K).

The magnetic and structural parameters of **1** and **2**, and previously reported[24] complexes Ni^{II}−Ni^{II}−Ni^{II} [d^8 ($S = 1$)−d^8 ($S = 1$)−d^8 ($S = 1$)] **3**, Ni^{II}−Mn^{II}−Ni^{II} **4**, and Ni^{II}−Co^{II}−Ni^{II} **5** are compared in Table 4. For the purpose of comparison, the magnetic results for **3**−**5** are presented here: $g_{iso} = 2.18$, J(Ni−Ni) = +1.10 cm^{-1}, and D = +3.49 cm^{-1} (for **3**); g(Ni) = 2.09(1), g(Mn) = 2.0 (fixed); J(Ni−Mn) = −0.30(1) cm^{-1} and D (for Ni^{II}) = +3.49 cm^{-1}; g(Ni) = 2.20(1), J(Ni−Co) = +1.06(3) cm^{-1}, $\lambda = -112(2)$ cm^{1}, $\alpha = kA = 1.30(1)$ (for **5**). In essence, out of five homo- and heterotrinuclear systems considered here, two homo- Co^{II}−Co^{II}−Co^{II} and Ni^{II}−Ni^{II}−Ni^{II} and three heterotrinuclear Co^{II}−Mn^{II}−Co^{II}, Ni^{II}−Mn^{II}−Ni^{II}, and Ni^{II}−Co^{II}−Ni^{II} complexes are ferromagnetically coupled with J values ranging between +1.20 and +0.71 cm^{-1}. The only system to exhibit effectively antiferromagnetic interaction ($J = -0.30$ cm^{-1}) is Ni^{II}−Mn^{II}−Ni^{II} complex. The most notable outcome of this investigation is to identify the measurable change in the nature and extent of magnetic-exchange interaction that occur due to a change in the M^{II} ion for a group of triply bridged trinuclear complexes, supported by invariant bridging characteristics.

Rationalization of Observed Magnetic Behavior in Terms of Structural Parameters. Unlike hydroxo- and alkoxo-bridged Cu^{II} dimers, systematic studies aimed at meaningful magnetostructural correlations/trends are less common in Ni^{II} complexes, due to fewer numbers of known complexes and to the large number of structural parameters that affect the superexchange mechanism in Ni^{II} systems. For di- or trinuclear Ni^{II} complexes,[39] the ferromagnetic interaction is observed for Ni−O−Ni angles lower than 93.5° (magic angle).[14] The coupling becomes antiferromagnetic for greater values. For other metal ions or heteropolynuclear complexes, this dependence is quite unknown. Moreover, it is possible that the magic angle may be lower than 93.5° for other metal ions such as Mn^{II} or Co^{II}. On the other hand, the carboxylate functionality can offer a variety of magnetic interactions depending on its versatile bridging modes syn−syn, syn−anti, and anti−anti. Generally, significant antiferromagnetic interaction between the metal centers is mediated by the syn−syn and anti−anti carboxylate coordination modes, whereas syn−anti mode mediates either weak ferro or antiferromagnetic interaction.

To understand the magnetic-exchange mechanism, it is important to note that complexes **1**−**5** have two monatomic bridges (from μ_2-1,1-acetate and μ_2-phenoxide) and a syn−syn μ_2-1,3-acetate bridge. For this last bridge, it is well-known that its presence brings about antiferromagnetic coupling.[1] Notably, the nature of magnetic interaction is dependent on the planarity of M_2O_2 core and M−O−M bond angle for the monatomic bridge. The deviation from planarity in M_2O_2 core causes poor orbital overlap between the metal orbital and the bridging ligand orbital, which in turn reduces antiferromagnetic coupling between interacting metal ions. Figure 5 depicts the non-planarity of the M_2O_2 core and the deviation (∼0.6 Å) of the terminal metal ion from the basal plane of the central metal ion, as observed in **1**−**5**. The dependence on bond angle has been

Table 4. Magnetic and Structural Parameters of μ_2-Phenoxo-, μ_2-1,1-Acetato-, and μ_2-1,1-Acetato-Bridged Homo- and Heterotrimers

complex no.	M−O M′−O (μ_2-phenoxo) (Å)	M−O M′−O (μ_2-1,1-OAc) (Å)	M−O M′−O (μ_2-1,3-OAc) (Å)	M−O−M′ (μ_2-phenoxo) (deg)	M−O−M′ (μ_2-1,1-OAc) (deg)	J (cm^{-1})
1[a]	2.0028(18) 2.0716(18)	2.1884(19) 2.1678(18)	2.0829(19) 2.0530(19)	101.864(18)	93.141(16)	+1.20
2[a]	2.006(3) 2.106(3)	2.190(3) 2.194(3)	2.088(3) 2.094(3)	101.623(17)	93.289(15)	+0.71(1)
3[b]	1.997(2) 2.049(2)	2.148(2) 2.117(2)	2.050(2) 2.016(2)	101.755(16)	94.794(15)	+1.10
4[b]	1.988(4) 2.095(4)	2.136(4) 2.197(4)	2.078(4) 2.144(4)	102.328(3)	94.441(3)	−0.30(1)
5[b]	2.004(3) 2.060(4)	2.132(4) 2.177(4)	2.064(4) 2.045(4)	102.110(4)	94.380(4)	+1.06(3)
$[Ni^{II}_3(L)_2(OBz)_4]$[c]	2.045(3) 2.062(13)	2.141(3) 2.115(3)	1.996(3)	94.61(9)	90.35(9)	+6.14(2)

[a]This work. [b]Reference 24. [c]Reference 16.

dx.doi.org/10.1021/ic302259t | Inorg. Chem. 2013, 52, 4825−4833

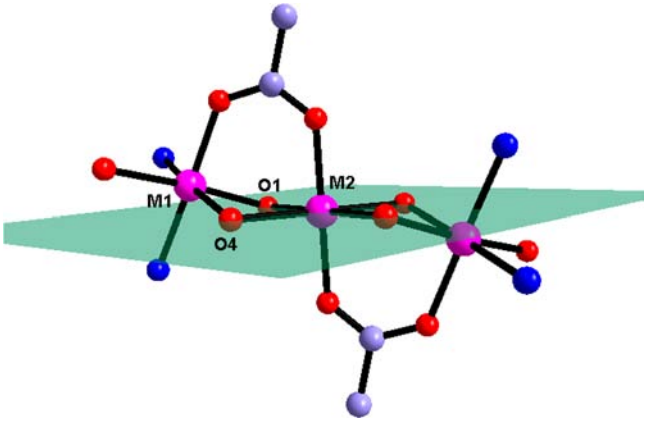

Figure 5. General representation of a plane passing through the basal plane of the central metal ion and deviation of the terminal metal ion from this plane.

well-studied for Cu^{II} dinuclear complexes, in contrast to scarce studies for other metal ions.[1] Given that the bond angles of **1**−**5** are greater than 93.5° (∼102° for μ_2-phenoxide and ∼94.5° for μ_2-1,1-acetate) and taking into account the above comments, an antiferromagnetic coupling for **1**−**5** would be expected. However, when the bridging ligands are different, the two bridges may either add (complementarity) or counterbalance (countercomplementarity) their effects.[22,23] It has been shown that the syn−syn μ_2-1,3-carboxylate and monatomic μ_2-1,1-azide bridges are countercomplementary and hence the antiferromagnetic contributions of each bridge cancel each other, and the ferromagnetic term dominates.[40] This situation is observed for **1**, **2**, **3**, and **5**, whereas in the case of **4**, the cancellation is not complete and a very weak antiferromagnetic contribution remains. A comparison along structures **1**−**5** reveals that, despite many other structural parameters, the metal−ligand bonding parameters within the bridging framework play a proactive role in determining the nature and strength of *J* values. More comparisons on the structural and magnetic parameters of the compounds in Table 4 can result in the same conclusion that the ferromagnetic interaction and the relative extent of ferromagnetic interaction arise due to composite effects of several structural parameters. Notably, the angle dependence Broken Symmetry Density Functional Theory (DFT) calculations reveal that the variation of the M−O(phenoxo)−M′ bond angle has a profound influence on the magnetic-exchange interaction than the monatomic carboxylate bridging.[3i] In this sense, for tri-μ_2-phenoxide-bridged trinuclear complexes of formula M_3L_2 (LH_3 = P(S)[N(Me)NdCHC$_6$H$_4$-*o*-O] and M = Ni^{II}, Co^{II}, and Mn^{II}), which present M−O−M angles in the range 85−87°, ferro- (Ni^{II} complex) and antiferromagnetic (Co^{II} and Mn^{II} complexes) interactions were observed.[11b]

CONCLUSION

In summary, we have demonstrated that by using the ligand L^- it has been possible to construct a group of five linear trinuclear complexes, comprising a similar terminal coordination environment ($M^{II}N_2O_4$: a tertiary amine N, a pyridyl N, a μ_2-phenoxide O, a μ_2-1,1-acetate O, a μ_2-1,3-acetate O, and a MeOH) around Ni^{II} ion or Co^{II} ion, variable central ion (Mn^{II}, Co^{II}, Ni^{II}) with $M^{II}O_6$ coordination environment, and invariant nature and number (two μ_2-phenoxido, two μ_2-1,3-acetato, and two μ_2-1,3-acetato) of bridging ligand interactions. In four complexes $Ni^{II}_2M^{II}$ (M = Co and Ni) and $Co^{II}_2M^{II}$ (M = Mn and Co) ferromagnetic and in $Ni^{II}_2Mn^{II}$ antiferromagnetic interactions are observed between neighboring metal ions. The linear trinuclear complexes provide examples of borderline cases of antiferro- and ferromagnetic coupling and reveal that even a small perturbation in structural parameters can lead to a change in the nature of coupling between the adjacent metal centers. The tunable magnetic interactions arise from controlled variation of the spin-state of the terminal M^{II} ion (Co, S = 3/2; Ni, S = 1) and the central M^{II} ion (Mn, S = 5/2; Co, S = 3/2; Ni, S = 1) giving rise to magnetic interactions involving variable spins. This study showed that judicious combination of terminal and bridging ligand affording invariant terminal and central metal ion coordination environment is a useful approach for the construction of a series of linear trinuclear complexes with tunable ground spin-states. While it appears that the ligand L^- should be able to generate trinuclear metal assemblies with many other metal ions in their bivalent oxidation state, this needs to be tested, and such efforts are underway in this laboratory.

ASSOCIATED CONTENT

Supporting Information

X-ray crystallographic files in CIF format, experimental and simulated X-ray powder diffraction patterns (Figures S1−S2); UV−vis spectra of **1**, **2**, and **6** (Figures S3−S5); perspective view of the metal coordination environment in the crystal of **1** (Figure S6); crystal packing diagrams of **1**−**6** (Figures S7−S12); and hydrogen-bonding parameters for **1**−**6** in Table S1. This material is available free of charge via the Internet at http://pubs.acs.org.

AUTHOR INFORMATION

Corresponding Author

*Phone: +91-512-2597437. Fax: +91-512-2597436. E-mail: rnm@iitk.ac.in.

Present Address

[§]Indian Institute of Science Education and Research, Kolkata Mohanpur Campus, Mohanpur 741 252, India.

Notes

The authors declare no competing financial interest.

ACKNOWLEDGMENTS

This work was supported by the Department of Science & Technology (DST), Government of India, and by the Ministerio de Educación y Ciencia. R.M. sincerely thanks the DST for a J. C. Bose fellowship. A.K.S. gratefully acknowledges the award of JRF and SRF by CSIR. We thank Amit Rajput for his help during revision of this manuscript.

REFERENCES

(1) Kahn, O. *Molecular Magnetism*; VCH: New York, 1993.
(2) (a) Oshio, H.; Nakano, M. *Chem.-Eur. J.* **2005**, *11*, 5178−5185. (b) Coronado, E.; Dunbar, K. R. *Inorg. Chem.* **2009**, *48*, 3293−3295. (c) Gatteschi, D.; Cornia, A.; Mannini, M.; Sessoli, R. *Inorg. Chem.* **2009**, *48*, 3408−3419. (d) Powell, A. K. *Nat. Chem.* **2010**, *2*, 351−352.
(3) (a) Crawford, V. H.; Richardson, H. W.; Wasson, J. R.; Hodgson, D. J.; Hatfield, W. E. *Inorg. Chem.* **1976**, *15*, 2107−2110. (b) Merz, L.; Haase, W. *J. Chem. Soc., Dalton Trans.* **1980**, 875−879. (c) Handa, M.; Koga, N.; Kida, S. *Bull. Chem. Soc. Jpn.* **1988**, *61*, 3853−3857. (d) Meenakumari, S.; Tiwari, S. K.; Chakravarty, A. R. *J. Chem. Soc., Dalton Trans.* **1993**, 2175−2181. (e) Nanda, K. K.; Thompson, L. K.; Bridson, J. N.; Nag, K. *J. Chem. Soc., Chem. Commun.* **1994**, 1337−

1338. (f) Thompson, L. K.; Mandal, S. K.; Tandon, S. S.; Bridson, J. N.; Park, M. K. *Inorg. Chem.* **1996**, *35*, 3117−3125. (g) Karmakar, T. K.; Ghosh, B. K.; Usman, A.; Fun, H.-K.; Rivière, E.; Mallah, T.; Aromí, G.; Chandra, S. K. *Inorg. Chem.* **2005**, *44*, 2391−2399. (h) Venegas-Yazigia, D.; Aravena, D.; Spodine, E.; Ruiz, E.; Alvarez, S. *Coord. Chem. Rev.* **2010**, *254*, 2086−2095. (i) Giri, S.; Biswas, R.; Ghosh, A.; Saha, S. K. *Polyhedron* **2011**, *30*, 2717−2722. (j) Sasmal, S.; Hazra, S.; Kundu, P.; Dutta, S.; Rajaraman, G.; Sañudo, E. C.; Mohanta, S. *Inorg. Chem.* **2011**, *50*, 7257−7267.

(4) (a) Verdaguer, M. *Polyhedron* **2001**, *20*, 1115−1128. (b) Christou, G. *Polyhedron* **2005**, *24*, 2064−2075.

(5) Arora, H.; Mukherjee, R. *New J. Chem.* **2010**, *34*, 2357−2365.

(6) (a) Escuer, A.; Aromí, G. *Eur. J. Inorg. Chem.* **2006**, 4721−4736. (b) Zeng, Y.-F.; Hu, X.; Liu, F.-C.; Bu, X.-H. *Chem. Soc. Rev.* **2009**, *38*, 469−480.

(7) (a) Arora, H.; Lloret, F.; Mukherjee, R. *Inorg. Chem.* **2009**, *48*, 1158−1167. (b) Arora, H.; Lloret, F.; Mukherjee, R. *Dalton Trans.* **2009**, 9759−9769. (c) Arora, H.; Lloret, F.; Mukherjee, R. *Eur. J. Inorg. Chem.* **2009**, 3317−3325. (d) Arora, H.; Cano, J.; Lloret, F.; Mukherjee, R. *Dalton Trans.* **2011**, *40*, 10055−10062.

(8) Bis-acetate (μ_2-1,3-mode) and μ_2-1,1-bridged M^{II}_3 (M = Mn, Co): Reynolds, R. A.; Dunham, W. R.; Coucouvanis, D. *Inorg. Chem.* **1998**, *37*, 1232−1241.

(9) Bis-acetate/benzoate (μ_2-1,1- and μ_2-1,3-modes)-bridged Co^{II}_3 complexes: (a) Catterick (née Drew), J.; Hursthouse, M. B.; New, D. B.; Thornton, P. *J. Chem. Soc., Chem. Commun.* **1974**, 843−844. Terminal Co^{II} centers assume tetrahedral geometry: (b) Ye, B.-H.; Chen, X.-M.; Xue, F.; Ji, L.-N.; Mak, T. C. W. *Inorg. Chim. Acta* **2000**, *299*, 1−8.

(10) Benzoate (μ_2-1,1- and μ_2-1,3-modes)-bridged complexes, (a) Co^{II}_3 (terminal Co^{II} centers assume distorted trigonal bipyramidal geometry) and $Ni^{II}_2Mn^{II}$: Gavrilenko, K. S.; Punin, S. V.; Cador, O.; Golhen, S.; Ouahab, L.; Pavlishchuk, V. V. *J. Am. Chem. Soc.* **2005**, *127*, 12246−12253. (b) Co^{II}_3 and $Co^{II}_2Mn^{II}$ (terminal Co^{II} centers in both complexes assume distorted trigonal bipyramidal geometry): Gavrilenko, K. S.; Le Gal, Y.; Cador, O.; Golhen, S.; Ouahab, L. *Chem. Commun.* **2007**, 280−282.

(11) Tris-μ_2-phenolate-bridged M^{II}_3 complexes, (a) M = Ni: Ohta, H.; Harada, K.; Irie, K.; Ka shino, S.; Kambe, T.; Sakane, G.; Shibahara, T.; Takamizawa, S.; Mori, W.; Nonoyama, M.; Hirotsu, M.; Kojima, M. *Chem. Lett.* **2001**, 842−843. (b) M = Mn, Co, Ni, Zn: Chandrasekhar, V.; Azhakar, R.; Senthil Andavan, G. T.; Krishnan, V.; Zacchini, S.; Bickley, J. F.; Steiner, A.; Butcher, R. J.; Kögerler, P. *Inorg. Chem.* **2003**, *42*, 5989−5998. (c) M = Ni: Heinicke, J.; Peulecke, N.; Karaghiosoff, K.; Mayer, P. *Inorg. Chem.* **2005**, *44*, 2137−2139.

(12) Tris-μ_2-phenolate-bridged $Ni^{II}_2Mn^{II}$ and $Ni^{II}_2Fe^{III}$ complexes: Kobayashi, T.; Yamaguchi, T.; Ohta, H.; Sunatsuki, Y.; Kojima, M.; Re, N.; Nonoyama, M.; Matsumoto, N. *Chem. Commun.* **2006**, 1950−1952.

(13) Tris-μ_2-phenolate/thiolate-bridged Ni^{II}_3/$Ni^{II}_2Ni^{III}$/$Ni^{III}_2Ni^{II}$ complexes: Beissel, T.; Birkelbach, F.; Bill, E.; Glaser, T.; Kesting, F.; Krebs, C.; Weyhermüller, T.; Wieghardt, K.; Butzlaff, C.; Trautwein, A. X. *J. Am. Chem. Soc.* **1996**, *118*, 12376−12390.

(14) Bis-μ_2-phenolate-bridged Ni^{II}_3 complex: Bu, X.-H.; Du, M.; Zhang, L.; Liao, D.-Z.; Tang, J.-K.; Zhang, R. -H.; Shionoya, M. *J. Chem. Soc., Dalton Trans.* **2001**, 593−598.

(15) Bis-μ_2-phenolate and μ_2-1,1-/μ_2-1,3-acetate-bridged complexes, (a) Fe^{II}_3 and Co^{II}_3: Gerli, A.; Hagen, K. S.; Marzilli, L. G. *Inorg. Chem.* **1991**, *30*, 4673−4676. (b) $Ni^{II}_2Cd^{II}$: Ülkü, D.; Tahir, M. N.; Atakol, O.; Nazir, H. *Acta Crystallogr.* **1997**, *C53*, 872−874. (c) Ni^{II}_3: Ülkü, D.; Ercan, F.; Atakol, O.; Dinçer, F. N. *Acta Crystallogr.* **1997**, *C53*, 1056−1057. (d) $Ni^{II}_2Mn^{II}$: Ercan, F.; Atakol, O. *Acta Crystallogr.* **1998**, *C54*, 1268−1270. (e) Ni^{II}_3: Reglinski, J.; Morris, S.; Stevenson, D. E. *Polyhedron* **2002**, *21*, 2167−2174. (f) Ni^{II}_3: Akine, S.; Nabeshima, T. *Inorg. Chem.* **2005**, *44*, 1205−1207.

(16) μ_2-Phenolate, μ_2-1,1-benzoate/cinnamate, and μ_2-1,3-benzoate/cinnamate Ni^{II}_3 complexes: Mukherjee, P.; Drew, M. G. B.; Gómez-García, C. J.; Ghosh, A. *Inorg. Chem.* **2009**, *48*, 5848−5860.

(17) μ_2-Phenolate, μ_2-1,3-acetate, and μ_2-1,1-azide Ni^{II}_3 complex: Biswas, R.; Mukherjee, S.; Kar, P.; Ghosh, A. *Inorg. Chem.* **2012**, *51*, 8150−8160.

(18) μ_2-Phenolate, μ_2-1,1-azide, and nitrate-bridged Cu^{II}_3: Biswas, C.; Drew, M. G. B.; Ruiz, E.; Estrader, M.; Diaz, C.; Ghosh, A. *Dalton Trans.* **2010**, *39*, 7474−7484.

(19) Bis-μ_2-phenolate and μ_2-1,3-acetate-bridged $Co^{III}_2Co^{II}$ complexes: (a) Chattopadhyay, S.; Bocelli, G.; Musatti, A.; Ghosh, A. *Inorg. Chem. Commun.* **2006**, *9*, 1053−1057. (b) Chattopadhyay, S.; Drew, M. G. B.; Ghosh, A. *Eur. J. Inorg. Chem.* **2008**, 1693−1701.

(20) Bis-μ_2-phenolate- and nitrito-bridged $Ni^{II}_2M^{II}$ (M = Mn, Co, Cu) complexes: Ercan, F.; Atakol, O.; Arici, C.; Svoboda, I.; Fuess, H. *Acta Crystallogr.* **2002**, *C58*, m193−m196.

(21) Bis-μ_2-1,3-$CF_3CO_2^-$ and hydroxamate-bridged Co^{II}_3 complex: Brown, D. A.; Clarkson, G. J.; Fitzpatric, N. J.; Glass, W. K.; Hussein, A. J.; Kemp, T. J.; Müller-Bunz, H. *Inorg. Chem. Commun.* **2004**, *7*, 495−498.

(22) Nishida, Y.; Kida, S. *J. Chem. Soc., Dalton Trans.* **1986**, 2633−2644.

(23) McKee, V.; Zvagulis, M.; Reed, C. A. *Inorg. Chem.* **1985**, *24*, 2914−2919.

(24) Sharma, A. K.; Lloret, F.; Mukherjee, R. *Inorg. Chem.* **2007**, *46*, 5128−5130.

(25) Karlin, K. D.; Cohen, B. I.; Hayes, J. C.; Farooq, A.; Zubieta, J. *Inorg. Chem.* **1987**, *26*, 147−153.

(26) Yajima, T.; Shimazaki, Y.; Ishigami, N.; Odani, A.; Yamauchi, O. *Inorg. Chim. Acta* **2002**, *337*, 193−202.

(27) O'Connor, C. J. *Prog. Inorg. Chem.* **1982**, *29*, 203−283.

(28) Farrugia, L. J. *WinGX ver 1.64, An Integrated Systems of Windows Programs for the Solution, Refinement and Analysis of Single-Crystal X-ray Diffraction Data*; Department of Chemistry, University of Glasgow: UK, 2003.

(29) Cotton, F. A.; Wilkinson, G.; Bochmann, M. *Advanced Inorganic Chemistry*, 6th ed.; Wiley: New York, 1999.

(30) Singh, S.; Mishra, V.; Mukherjee, J.; Seethalekshmi, N.; Mukherjee, R. *Dalton Trans.* **2003**, 3392−3397.

(31) (a) Mandal, S.; Balamurugan, V.; Lloret, F.; Mukherjee, R. *Inorg. Chem.* **2009**, *48*, 7544−7556. (b) Arora, H.; Barman, S. K.; Lloret, F.; Mukherjee, R. *Inorg. Chem.* **2012**, *51*, 5539−5553.

(32) Brammer, L., Desiraju, G. R., Eds. *Perspectives in Supramolecular Chemistry − Crystal Design: Structure and Function*; Wiley: Chichester, 2003; Vol. 7, pp 1−75.

(33) Balamurugan, V.; Hundal, M. S.; Mukherjee, R. *Chem.-Eur. J.* **2004**, *10*, 1683−1690.

(34) (a) Figgis, B. N.; Gerloch, M.; Lewis, J.; Mabbs, F. E.; Webb, G. A. *J. Chem. Soc. A* **1968**, 2086−2093. (b) Gerloch, M.; Quested, P. N. *J. Chem. Soc. A* **1971**, 3729−3741.

(35) Mabbs, F. E.; Machin, D. J. *Magnetism in Transition Metal Complexes*; Chapman and Hall: London, 1973.

(36) Mishra, V.; Lloret, F.; Mukherjee, R. *Inorg. Chim. Acta* **2006**, *359*, 4053−4062 and references therein.

(37) Lloret, F.; Julve, M.; Cano, J.; Ruiz-Garćia, R.; Pardo, E. *Inorg. Chim. Acta* **2008**, *361*, 3432−3445.

(38) Zhao, Q.; Li, H.; Chen, Z.; Fang, R. *Inorg. Chim. Acta* **2002**, *336*, 142−146 and references therein.

(39) Ginsberg, A. P.; Martin, R. L.; Sherwood, R. C. *Inorg. Chem.* **1968**, *7*, 932−936.

(40) Thompson, L. K.; Tandon, S. S.; Lloret, F.; Cano, J.; Julve, M. *Inorg. Chem.* **1997**, *36*, 3301−3306.